Bosonic, fermionic, and anyonic symmetry in two-photon random scattering

M. P. van Exter, J. Woudenberg, H. Di Lorenzo Pires, and W. H. Peeters
Huygens Laboratory, Leiden University, P.O. Box 9504, 2300 RA Leiden, The Netherlands
(Received 20 September 2011; published 21 March 2012)

We experimentally demonstrate the importance of two-photon symmetry for the propagation of spatial quantum correlations in a multiple-scattering disordered system. Two distinguishable entangled photons with tunable spatial exchange symmetry are sent through the scattering medium. The two photons are observed to have an ensemble-averaged tendency to cluster together (bosonic symmetry) or to avoid each other (fermionic symmetry). An intermediate degree of clustering is observed for anyonic exchange symmetry.

DOI: 10.1103/PhysRevA.85.033823 PACS number(s): 42.50.Ar, 42.25.Dd, 42.30.Ms, 42.50.Dv

I. INTRODUCTION

Symmetry plays a crucial role in the description of multiparticle systems. This is common knowledge in solid-state physics, but it is less known in optics. In quantum optics, the most prominent example of the importance of symmetry is the occurrence of photon bunching in two-photon interference. Hong, Ou, and Mandel were the first to show that when two identical photons are combined on a beamsplitter they always leave via the same output channel and never choose different channels [1]. Later experiments with photons that were distinguishable by their polarization have shown how the symmetry of the two-particle wave function can be changed and how the two-particle interference changes accordingly from photon bunching to antibunching. The first quantum interference experiments were performed with an ordinary beamsplitter, with two input and two output channels [2–4].

Recent experiments have extended the number of available spatial channels and studied the evolution of the full spatial wave function upon propagation through a two-dimensional maze of beamsplitters, built from coupled waveguides. After the first so-called quantum walk experiments with classical light [5], it was quickly suggested to use quantum-entangled photon pairs as input and study the resulting quantum correlations between the numerous output channels [6]. In 2010, the first quantum-correlated random walk was demonstrated for a symmetric two-photon input [7]. In 2012, the symmetry of the input state was modified and the two-particle random walk was also studied with states with different symmetry [8]. The number of input channels in all mentioned experiments was limited to either 2 or 3.

This paper adds two aspects to the discussion. First, we experimentally demonstrate two-particle quantum interference for a much larger geometry that comprises typically ≈ 100 spatial input modes and a comparable number of output modes. Second, our geometry is truly random, being based on naturally occurring scattering in disordered systems. This fact, among others, allows us to average over multiple-scattering geometries and extract important statistical information on the (symmetry of the) two-particle interference.

Coherent scattering in random media has attracted lots of interest on account of its intriguing physics, which includes speckle formation [9], conductance fluctuations [10,11], enhanced backscattering [12], and indications of Anderson localization [13]. Multiparticle effects have been studied via the propagation of quantum noise and quantum entanglement through random media [14–18]. Symmetry aspects in multiparticle scattering have not yet been explored.

This paper demonstrates the role of symmetry on the propagation of two distinguishable photons through a multiply scattering random medium. We regard the full spatial structure of a multimode entangled photon pair (typically $N \approx 100$ spatial modes). In essence, our scattering medium acts as an $N \times N$ multimode random beamsplitter that coherently redistributes the spatial information but does not affect the polarization labeling that makes our photons distinguishable. We can tune the spatial exchange symmetry of the photons such that they mimic the intrinsic symmetries of bosons, fermions, and anyons. These experiments demonstrate that this symmetry strongly affects the spatial quantum correlations after propagation through the disordered scatterer, even after ensemble averaging.

A central concept in our theoretical description is the two-photon field $A_{HV}(\boldsymbol{\rho}_1,\boldsymbol{\rho}_2) = \langle 0|\hat{a}_H(\boldsymbol{\rho}_1)\hat{a}_V(\boldsymbol{\rho}_2)|\Psi\rangle$, where $\hat{a}$ is the photon annihilation operator and $|\Psi\rangle$ is the optical quantum state. The two-photon field $A_{HV}(\boldsymbol{\rho}_1,\boldsymbol{\rho}_2)$ is the probability amplitude to observe the H-polarized photon at transverse position $\boldsymbol{\rho}_1$ and the V-polarized photon at $\boldsymbol{\rho}_2$. We will first study the evolution of an input two-photon field with the natural bosonic symmetry $A_{HV}(\boldsymbol{\rho}_1,\boldsymbol{\rho}_2) = A_{HV}(\boldsymbol{\rho}_2,\boldsymbol{\rho}_1)$. Next, we introduce an experimental technique that allows us to tune the particle exchange symmetry. For an antisymmetric input field $A_{HV}(\boldsymbol{\rho}_1,\boldsymbol{\rho}_2) = -A_{HV}(\boldsymbol{\rho}_2,\boldsymbol{\rho}_1)$, we observe photon antibunching in the output channels where the photons try to avoid each other and never scatter into identical spatial modes. For anyonic symmetry, we observe how the exchange interaction between the two photons combines effective attraction with repulsion.

II. EXPERIMENT: BOSONIC SYMMETRY

Figure 1 shows the experimental setup. Quantum-entangled photon pairs with orthogonal H and V polarization are generated in the nonlinear optical process of spontaneous parametric down-conversion (SPDC), where a single pump photon occasionally splits up into two photons [19]. We use a 5-mm-long periodically poled KTP crystal and a 200 mW cw single-mode beam from a krypton ion laser operating at a wavelength of 413 nm and focused to a waist $w \approx 150\ \mu$m, thus generating $N \approx 100$ spatial modes [20]. The pump light is removed with an antireflective-coated GaP wafer positioned behind the KTP crystal, while the frequency-degenerate photon pairs are

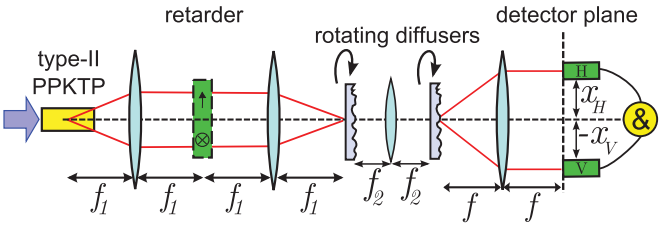

FIG. 1. (Color online) Experimental setup. From left to right: quantum-entangled photon pairs pass through an optional retarder (to tailor the spatial two-photon symmetry) and scatter from a random medium, comprising two rotating diffusors, before being detected by two photon counters and coincidence logic.

selected with narrow-band interference filters ($\Delta\lambda = 1$ nm at $\lambda \approx 826$ nm). The symmetry of the input two-photon field can be modified by an optional custom-made retarder plate, to be discussed below. The photon pairs generated are focused onto a scattering medium comprising two random phase plates (scattering angle 1°) positioned in conjugate planes [16]. Both plates are continuously rotated to allow ensemble averaging. The spatial correlation of the scattered photons is measured with two single-photon detectors, located in the far field of the scattering medium and connected to fast electronics that record both individual and coincidence counts. A polarizing beamsplitter (not shown) separates the scattered H and V photons before detection and allows us to position the two detectors effectively on top of each other. Each detector is connected to a single-mode optical fiber, whose compact image (140 μm) can be scanned in the far-field plane of the scattering medium. All scans are (for the moment) limited to the x direction, keeping $y_H = y_V = 0$ fixed [transverse coordinate $\boldsymbol{\rho} = (x, y)$].

The image on the left-hand side of Fig. 2 shows the experimental result obtained without a retarder. This false-color plot depicts the coincidence rate $\overline{R_{cc}(x_H, x_V)} \propto \overline{|A_{HV}(x_H, x_V)|^2}$ as a function of the transverse positions x_H and x_V of the H- and V-polarized photon in the detector plane, where the bar denotes ensemble averaging. Previous correlation measurements on a stationary scattering medium exhibited two-photon speckle in the absence of one-photon speckle (see Figs. 3 and 4(c) in Ref. [16]). Being interested in ensemble-averaged pair correlations only, we now apply a sample rotation to average over many ($\gg$100) speckle patterns. This removes most features from the two-photon speckle, apart from a prominent enhancement along the diagonal $x_H = x_V$. All discussed two-photon features are observed in the absence of one-photon speckle, at approximately constant single-photon count rate, and after subtraction of a small fraction ($\approx 10\%$) of accidental coincidence counts. Integration times are typically 12 s per date point.

The enhanced coincidence rate observed along the $x_H = x_V$ diagonal is the photon bunching that we wish to study. For a quantitative analysis, we select data within a rectangular box oriented at 45° and project and average the data along this direction. The upper (blue) curve in the central image of Fig. 2 shows the projected coincidence rate as a function of the position difference $x_H - x_V$. Photon bunching is observed as an increase of the coincidence rate around $x_H - x_V \approx 0$ by a bunching factor $F \equiv \overline{R_{cc}(x_H = x_V)}/\overline{R_{cc}(x_H \neq x_V)} = 1.90 \pm 0.03$ with respect to neighboring values. This is close to the value of 2 expected from the bosonic symmetry of the incident two-photon field, as discussed below. The width of the bunching peak (FWHM $= 0.54 \pm 0.02$ mm for a high-quality Gaussian fit) denotes the size of a spatial mode. It is comparable to the size of the two-photon speckles observed for a static (nonrotating) sample and Fourier related to the average spot size of the two-photon illumination on the final diffusor [16].

III. EXPERIMENTS: MODIFIED SYMMETRY

Next, we discuss two-photon scattering of input states with a different symmetry. We modify this symmetry by passing the photon pairs through a custom-made retarder plate, comprising two identical zero-order retarders with retardation phase $\varphi/2$ that are rotated 90° with respect to each other and mounted side-by-side to fill two half-spaces ($x < 0$ and $x > 0$). Since the plate is positioned in the far field of the source and since the emission angles of the photons are anticorrelated, the two photons will generally pass through opposite plate segments. The retardation phases imposed by the retarder thereby modify

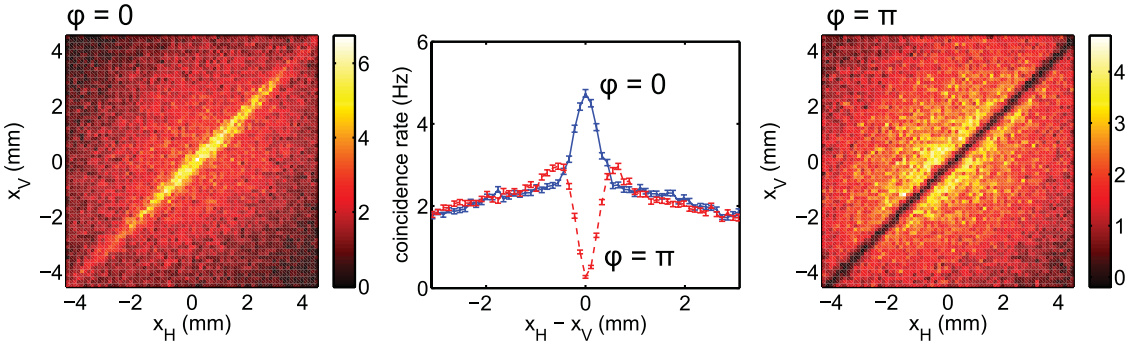

FIG. 2. (Color online) Observation of bosonic and fermionic symmetry in two-photon scattering. (Left, right) False-color plots of the coincidence count rate, observed in the far field of a random scattering medium, vs the detector positions x_H and x_V; the left figure is measured for a symmetric ($\varphi = 0$) two-photon input field; the right figure applies to the antisymmetric ($\varphi = \pi$) case. (Middle) Projected coincidence rate vs the position difference $x_H - x_V$. The upper (blue) $\varphi = 0$ curve exhibits photon bunching; the lower (red) $\varphi = \pi$ curve exhibits photon antibunching.

the bosonic symmetry of the incident field into a new symmetry

$$A_{\text{plate}}(\boldsymbol{\rho}_2,\boldsymbol{\rho}_1) = e^{i\varphi} A_{\text{plate}}(\boldsymbol{\rho}_1,\boldsymbol{\rho}_2) \tag{1}$$

for $x_1 > 0$ and $x_2 < 0$. We will neglect the weak field associated with photon pairs that do not split up, but instead both pass through the same plate segment; the probability of these rare pairs is ≈ 0.05 in our experiment. A similar trick with a segmented retarder plate has been used before to modify the two-photon coincidence pattern behind a double slit from spatial bunching to antibunching [21].

After modification, we again send the two-photon state through the multiple-scattering system that randomly mixes the positions of the photons. Despite this mixing, the symmetry between the two dominant contributions remains intact throughout the system. An essential requirement for this, is that the propagation and scattering are polarization insensitive, as is (practically) the case in our paraxial geometry with small scattering angles. The combined two-photon field in any transverse plane that follows can thus be written as

$$A_{HV}(\boldsymbol{\rho}_1,\boldsymbol{\rho}_2) \approx A_q(\boldsymbol{\rho}_1,\boldsymbol{\rho}_2) + e^{i\varphi} A_q(\boldsymbol{\rho}_2,\boldsymbol{\rho}_1)\,, \tag{2}$$

where $A_q(\boldsymbol{\rho}_1,\boldsymbol{\rho}_2)$ singles out the scattered field that originates from all photon pairs at positions $x_1 > 0$ and $x_2 < 0$ on the retarder plate. It is important to note that the spatial symmetry described by Eq. (2) is generally different from that described by Eq. (1). They are identical only for bosonic ($\varphi = 0$) and fermionic ($\varphi = \pi$) symmetry, where Eq. (2) reduces to $A_{HV}(\boldsymbol{\rho}_1,\boldsymbol{\rho}_2) = \pm A_{HV}(\boldsymbol{\rho}_2,\boldsymbol{\rho}_1)$ *in any transverse plane*. For the more general case ($\varphi \neq \{0,\pi\}$), we cannot rewrite Eq. (2) in a comparable form, due to the complex nature of $A_q(\boldsymbol{\rho}_1,\boldsymbol{\rho}_2)$. On these grounds, one might even state that the bosonic and fermionic symmetries are more robust than the anyonic symmetry in our experiment.

Figure 3 is a graphical representation of Eq. (2). It shows how the observed bunching effects originate from the interference of the field A_q with its mirror image. When the detectors are displaced with respect to each other ($\boldsymbol{\rho}_1 \neq \boldsymbol{\rho}_2$) these two contributions will generally differ and thus sum *incoherently* to the ensemble-averaged signal. At $\boldsymbol{\rho}_1 \approx \boldsymbol{\rho}_2$, however, the field propagators become identical and the two contributions add *coherently*. The two-photon coincidence rate at $\boldsymbol{\rho}_1 \approx \boldsymbol{\rho}_2$ will thus be enhanced by a factor $|1 + \exp(i\varphi)|^2/2 = 1 + \cos\varphi$ as compared to neighboring positions $\boldsymbol{\rho}_1 \neq \boldsymbol{\rho}_2$. Photon bunching occurs for the symmetric ($\varphi = 0$) two-photon input, while antibunching occurs for the antisymmetric ($\varphi = \pi$) input.

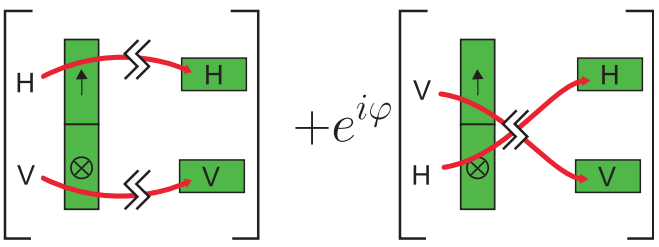

FIG. 3. (Color online) Graphical explanation of bunching effect. The observed bunching effects originate from the interference of two generic scattering paths of the photon pair from the retarder plane (left), via propagation and scattering (denoted by sharp ss symbols), to the detectors (right).

The image on the right-hand side of Fig. 2 is a false-color plot of the average coincidence rate $\overline{R_{\text{cc}}(x_H,x_V)}$ observed for an antisymmetric input field ($\varphi = \pi$). A drastic reduction of the coincidence count rate is now observed for all pairs around the diagonal $x_H = x_V$, irrespective of the individual values of x_H and x_V. We again select a rectangular box, project onto the diagonal, and plot the projected coincidence rate versus the position difference $x_H - x_V$. The lower (red) curve in the central image of Fig. 2 shows the occurrence of photon antibunching around $x_H \approx x_V$. The central minimum decreases to a bunching factor $F = 0.09 \pm 0.04$ of neighboring values, to be compared with an ideal value of 0. At a FWHM of 0.40 ± 0.02 μm, the central minimum is slightly narrower than the maximum observed under photon bunching and two small shoulders appear. We attribute the somewhat smaller width of the fermionic structure and its additional weak shoulder (a remnant of photon bunching) to the small contribution of photon pairs with $x_1.x_2 > 0$ in the retarder plane; a contribution that we previously neglected. Both aspects also show up in numerical calculations that simulate our system in one transverse dimension.

As a final experiment, we replace the $\varphi = \pi$ plate by a similar $\varphi = \pi/2$ retarder plate. This plate transforms the generated state into a two-photon field with the unusual symmetry $A_{\text{plate}}(x_2 < 0, x_1 > 0) = \exp(i\varphi) A_{\text{plate}}(x_1 > 0, x_2 < 0)$, where $\exp(i\varphi) = i$ for the considered $\varphi = \pi/2$. The symmetry of this state interpolates between bosonic and fermionic and can hence be called anyonic.

The term anyon was introduced by Wilczek [22] to describe the statistics of composite quasiparticles in a two-dimensional system, formed by charged particles and flux tubes. These composites behave as quasiparticles with fractional quantum statistic [22–24], as they acquire a phase factor $\pm\exp(i\varphi)$ upon exchange, where the sign depends on the sense of rotation around the vortex. Anyons are the key ingredient for topological quantum computing, where quantum information is stored in the topological structure of a quantum state [25,26]. Our experiment shows that anyonic symmetry is also relevant for the scattering statistics of entangled photon pairs.

Figure 4 shows the results obtained under illumination with a two-photon field with anyonic symmetry ($\varphi = \pi/2$). The two figures on the right-hand side are false-color plots of the coincidence count rate versus the detector positions. The main figure shows a diagonal projection of these data, using the method described earlier. The two wiggly (blue and black) curves are obtained for two different orientation of the retarder plate, where the front side of the plate was facing either the source or the scattering medium. These two curves are approximate mirror images, in agreement with the inversion ($\varphi \to -\varphi$) or ($x \to -x$) associated with the reorientation of the plate. Each curve demonstrates an intriguing combination of bunching and antibunching. The exchange interaction between the two photons is now asymmetric, such that the H-polarized photon prefers to be on the right-hand side of the V-polarized photon, but avoids the left-hand side for one orientation of the plate, and vice versa for the other orientation. This unusual asymmetry originates from the spatial structure of the A_q field at the second diffusor. It disappears at increased scattering angles and is absent if we scan the detectors in the

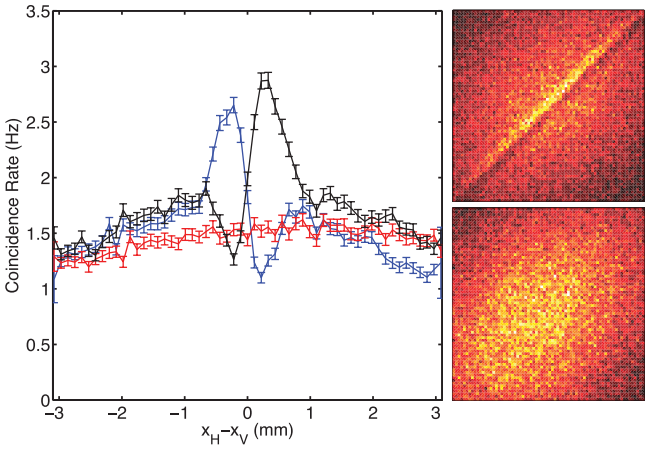

FIG. 4. (Color online) Observation of anyonic symmetry in two-photon scattering. (Left) Projected coincidence rate vs the position difference $x_H - x_V$ for an input field with anyonic symmetry. The two wiggly (blue and black) curves are measured for $\varphi = \pi/2$ and $\varphi = -\pi/2$, respectively. The nonwiggly (red) curve is measured while scanning in the orthogonal transverse direction $y_H - y_V$. (Right) False color plots of the coincidence count rate observed at $\varphi = \pi/2$ while scanning either in the (x_H, x_V) plane (top right) or in the (y_H, y_V) plane (bottom right). The scale of both figures is identical to that of Figs. 2(a) and 2(c).

orthogonal transverse direction $y_H - y_V$ (see red nonwiggly curve in Fig. 4).

IV. CONCLUDING DISCUSSION

In conclusion, we have shown that particle exchange symmetry plays a crucial role in two-photon scattering. Depending on the symmetry of the two-photon field of two distinguishable (H and V polarized) photons, we have observed spatial bunching, spatial antibunching, and mixed behavior, thus mimicking the behavior of bosons, fermions, and anyons. These bunching effects originate from the conservation of (a special form of) particle exchange symmetry.

From a general perspective, our experiments demonstrate the importance of exchange symmetry in multiparticle scattering. For the extreme cases of bosonic ($\varphi = 0$) and fermionic ($\varphi = \pi$) symmetry, this exchange symmetry applies to any $(\boldsymbol{\rho}_1, \boldsymbol{\rho}_2)$ combination and Eqs. (1) and (2) are equivalent. For intermediate symmetries ($0 < \varphi < \pi$) only the more general Eq. (2) applies. To quantify the exchange symmetry also for these cases, we introduce the global (spatially averaged) symmetry parameter

$$S \equiv \frac{\iint A^*(\boldsymbol{\rho}_2, \boldsymbol{\rho}_1) A(\boldsymbol{\rho}_1, \boldsymbol{\rho}_2)\, d\boldsymbol{\rho}_1 d\boldsymbol{\rho}_2}{\iint |A(\boldsymbol{\rho}_1, \boldsymbol{\rho}_2)|^2 d\boldsymbol{\rho}_1 d\boldsymbol{\rho}_2}. \tag{3}$$

This real-valued symmetry parameter S is conserved under unitary scattering and propagation if these processes are identical for both particles. The parameter S determines the bunching factor after random scattering via $F \approx 1 + S$. For our system $S = \cos\varphi$, with fermionic ($S = -1$) and bosonic ($S = 1$) symmetry as extreme cases. Similar exchange symmetries will be crucial in any future two-particle experiment.

ACKNOWLEDGMENTS

We thank J. P. Woerdman for fruitful discussions and acknowledge support from the Stichting voor Fundamenteel Onderzoek der Materie (FOM) and the EU under the FET-Open Agreement HIDEAS, No. FP7-ICT-221906.

[1] C. K. Hong, Z. Y. Ou, and L. Mandel, Phys. Rev. Lett. **59**, 2044 (1987).
[2] P. G. Kwiat, A. M. Steinberg, and R. Y. Chiao, Phys Rev. A **45**, 7729 (1992).
[3] S. P. Walborn, A. N. de Oliveira, S. Pádua, and C. H. Monken, Phys. Rev. Lett. **90**, 143601 (2003).
[4] T. Yarnall, A. F. Abouraddy, B. E. A. Saleh, and M. C. Teich, Phys. Rev. Lett. **99**, 250502 (2007); Phys. Rev. A **79**, 043817 (2009).
[5] H. B. Perets, Y. Lahini, F. Pozzi, M. Sorel, R. Morandotti, and Y. Silberg, Phys. Rev. Lett. **100**, 170506 (2008).
[6] Y. Bromberg, Y. Lahini, R. Morandotti, and Y. Silberg, Phys. Rev. Lett. **102**, 253904 (2009).
[7] A. Peruzzo *et al.*, Science **329**, 1500 (2010).
[8] L. Sansoni, F. Sciarrino, G. Vallone, P. Mataloni, A. Crespi, R. Ramponi, and R. Osellame, Phys. Rev. Lett. **108**, 010502 (2012).
[9] J. W. Goodman, J. Opt. Soc. Am. **66**, 1145 (1976).
[10] S. Washburn and R. A. Webb, Rep. Prog. Phys. **55**, 1311 (1992).
[11] C. W. J. Beenakker, Rev. Mod. Phys. **69**, 731 (1997).
[12] M. P. Van Albada and A. Lagendijk, Phys. Rev. Lett. **55**, 2692 (1985); *ibid.***56**, 1471 (1986).
[13] D. S. Wiersma, P. Bartolini, A. Lagendijk, and R. Righini, Nature **390**, 671 (1997); comment by F. Scheffold, R. Lenke, R. Tweer, and G. Maret and reply by D. S. Wiersma *et al.*, *ibid.* **398**, 206 (1999).
[14] C. W. J. Beenakker, J. W. F. Venderbos, and M. P. van Exter, Phys. Rev. Lett. **102**, 193601 (2009).
[15] P. Lodahl and A. Lagendijk, Phys. Rev. Lett. **94**, 153905 (2005).
[16] W. H. Peeters, J. J. D. Moerman, and M. P. van Exter, Phys. Rev. Lett. **104**, 173601 (2010).
[17] J. R. Ott, N. A. Mortensen, and P. Lodahl, Phys. Rev. Lett. **105**, 090501 (2010).
[18] Y. Lahini, Y. Bromberg, D. N. Christodoulides, and Y. Silberberg, Phys. Rev. Lett. **105**, 163905 (2010).
[19] P. G. Kwiat, K. Mattle, H. Weinfurter, A. Zeilinger, A. V. Sergienko, and Y. H. Shih, Phys. Rev. Lett. **75**, 4337 (1995).

[20] H. Di Lorenzo Pires, C. H. Monken, and M. P. van Exter, Phys. Rev. A **80**, 022307 (2009).
[21] W. A. T. Nogueira, S. P. Walborn, S. Pádua, and C. H. Monken, Phys. Rev. Lett. **86**, 4009 (2001).
[22] F. Wilczek, Phys. Rev. Lett. **49**, 957 (1982).
[23] R. B. Laughlin, Phys. Rev. Lett. **50**, 1395 (1983).
[24] B. I. Halperin, Phys. Rev. Lett. **52**, 1583 (1984); New J. Phys. **11**, 083010 (2009).
[25] G. K. Brennen and J. K. Pachos, Proc. R. Soc. A **464**, 1 (2008).
[26] C.-Y. Lu, W.-B. Gao, O. Gühne, X.-Q. Zhou, Z.-B. Chen, and J.-W. Pan, Phys. Rev. Lett. **102**, 030502 (2009); Nature **445**, 402 (2007); Rev. Mod. Phys. **71**, S306 (1999).